



THE UNIVERSITY *of* EDINBURGH

Edinburgh Research Explorer

Optimization of the visibility of graphene on poly-Si film by thin-film optics engineering

Citation for published version:

Chen, T, Mastropaolo, E, Bunting, A, Stevenson, T & Cheung, R 2012, 'Optimization of the visibility of graphene on poly-Si film by thin-film optics engineering', *Journal of Vacuum Science and Technology B*, vol. 30, no. 6, 06FJ01. <https://doi.org/10.1116/1.4758760>

Digital Object Identifier (DOI):

[10.1116/1.4758760](https://doi.org/10.1116/1.4758760)

Link:

[Link to publication record in Edinburgh Research Explorer](#)

Document Version:

Publisher's PDF, also known as Version of record

Published In:

Journal of Vacuum Science and Technology B

Publisher Rights Statement:

Publisher's Version/PDF: author can archive publisher's version/PDF

General rights

Copyright for the publications made accessible via the Edinburgh Research Explorer is retained by the author(s) and / or other copyright owners and it is a condition of accessing these publications that users recognise and abide by the legal requirements associated with these rights.

Take down policy

The University of Edinburgh has made every reasonable effort to ensure that Edinburgh Research Explorer content complies with UK legislation. If you believe that the public display of this file breaches copyright please contact openaccess@ed.ac.uk providing details, and we will remove access to the work immediately and investigate your claim.



Optimization of the visibility of graphene on poly-Si film by thin-film optics engineering

Tao Chen, Enrico Mastropaolo, Andrew Bunting, Tom Stevenson, and Rebecca Cheung

Citation: J. Vac. Sci. Technol. B 30, 06FJ01 (2012); doi: 10.1116/1.4758760

View online: <http://dx.doi.org/10.1116/1.4758760>

View Table of Contents: <http://avspublications.org/resource/1/JVTBD9/v30/i6>

Published by the AVS: Science & Technology of Materials, Interfaces, and Processing

Additional information on J. Vac. Sci. Technol. B

Journal Homepage: <http://avspublications.org/jvstb>

Journal Information: http://avspublications.org/jvstb/about/about_the_journal

Top downloads: http://avspublications.org/jvstb/top_20_most_downloaded

Information for Authors: http://avspublications.org/jvstb/authors/information_for_contributors

ADVERTISEMENT



The advertisement features a blue and yellow color scheme. On the left, a vertical blue bar contains the website address 'www.raith.com'. To its right, the text 'eLINE plus' is displayed in a stylized font. Below this, a list of capabilities is shown: 'fabricate', 'modify', 'manipulate', and 'measure', each preceded by a blue arrow. In the center, there is an image of the Raith eLINE plus system, which includes a computer monitor on a desk, a large white and blue machine unit, and a tall server rack. To the right of the machine, the text 'Nanoengineering beyond Electron Beam Lithography' is written in a bold, sans-serif font. At the bottom right, the 'Raith' logo is prominently displayed in a large, bold, yellow font, with the tagline 'INNOVATIVE SOLUTIONS FOR NANOFABRICATION' underneath it.

www.raith.com

eLINE plus

- ▶ fabricate
- ▶ modify
- ▶ manipulate
- ▶ measure

Nanoengineering
beyond
Electron Beam
Lithography

Raith
INNOVATIVE SOLUTIONS FOR
NANOFABRICATION

Optimization of the visibility of graphene on poly-Si film by thin-film optics engineering

Tao Chen,^{a)} Enrico Mastropaolo, Andrew Bunting, Tom Stevenson, and Rebecca Cheung
*Scottish Microelectronics Centre, The University of Edinburgh, King's Buildings, West Mains Road,
Edinburgh EH9 3JF, United Kingdom*

(Received 29 June 2012; accepted 24 September 2012; published 11 October 2012)

A multilayer optical system containing poly-Si film, SiO₂ film, and Si substrate (poly-Si substrate) has been designed to enhance the visibility of graphene in contact with poly-Si. Film thicknesses of poly-Si and SiO₂ have been optimized by parametric study of the integral contrast of single layer graphene using transfer matrix theory. The multilayer poly-Si substrate and the most commonly used 285 nm SiO₂/Si substrate (SiO₂ substrate) have been fabricated. Graphene grown by chemical vapor deposition on Ni catalyst has been transferred to the substrates and the visibility of the graphene on the different substrates has been compared. The samples have been characterized by optical microscope, illuminated with light from halogen lamp, and/or filtered with a 600 nm narrow band optical filter. The contrast of graphene on poly-Si substrate has been increased to near 8.7% under 600 nm narrow band illumination from nearly invisible under ordinary illumination, while the contrast of graphene on SiO₂ remains almost the same. Raman spectroscopy has been used to verify the presence of the single layer graphene on the poly-Si substrate. © 2012 American Vacuum Society. [<http://dx.doi.org/10.1116/1.4758760>]

I. INTRODUCTION

Since single layer graphene (SLG) has been found on 300 nm SiO₂/Si substrate for the first time,¹ it has drawn wide range of interests. Diversified devices based on graphene have been prototyped, including chemical sensors,² resonators,³ and MOSFETs.⁴ Graphene features high robustness, chemical inertness, and unrivaled electron and hole mobility.¹ The most promising applications of graphene include transparent electrodes, super capacitors, and RF transistors. However, some shortcomings have hindered the application of graphene.

The conduction band of graphene touches its valence band at Dirac point, thus no band-gap exists. Graphene channel cannot be shut down completely by field effect even when Fermi level coincides with Dirac point, which is the neutral point. However, the electron transport can be blocked in the channel by some novel mechanisms such as electron deflection by potential barrier.⁵ To induce a potential barrier, doping methods including electrostatic and chemical doping have been proposed. Organic substances have been reported to be able to dope graphene and the doping level is sensitive to some physical factors such as light illumination depending on the properties of the organics,⁶ which can be applied in sensors. Modulation doping is another possible way to dope graphene,⁷ which resembles chemical doping in principle. However, not many experimental results have been reported to verify the viability of modulation doping.

One of the possible ways to dope graphene by modulation doping is to put graphene on Si substrate, however, SLG will not be visible on a bare Si wafer, which will complicate the fabrication process. Therefore, we have designed a poly-Si/SiO₂/Si multilayer substrate and optimized the film thicknesses to enhance the visibility of graphene on top of poly-Si

surface, similar to the recent visibility study of SLG on GaAs substrate using a periodic structure.⁸ The development of such a substrate will facilitate the research of modulation doping of graphene by poly-Si. In addition, poly-Si is a widely used sacrificial material in micromachining. Visualization of the graphene on poly-Si will enable new fabrication process for graphene nanoelectromechanical systems (NEMS).

II. THEORY

A. Origin of high contrast

The single layer graphene is highly transparent, with its absorption rate being around 2.3%.⁹ Suppose a single layer graphene is placed on top of a monocrystalline silicon substrate, the contrast between the substrate and the graphene sheet will be too small to be distinguishable. As reported in the literature,^{10,11} a distinctive contrast under optical microscope comes from the difference between the reflectivity of the area with graphene on top and the rest of the substrate without graphene. To change the reflection significantly by just one layer of graphene, a thin dielectric film can be coated on the substrate to meet destructive interference condition [Fig. 1(a)], which is easily destroyed by the graphene layer [Fig. 1(b)].

However, the antireflection cannot be realized for poly-Si layer on Silicon substrate, since the refractive index of poly-Si is almost the same as crystalline Silicon. If the poly-Si is deposited on Si, their interface will not reflect light as depicted by Fresnel's Law. To achieve destructive interference condition for poly-Si film, it is necessary to insert a thin film with different refractive index between poly-Si and Si substrate. In consideration of process convenience, a SiO₂ layer has been chosen to enable the reflected light from the three interfaces shown in Fig. 1(c) to cancel each other as much as possible. Under this crucial condition, when a graphene is placed on

^{a)}Electronic mail: t.chen@ed.ac.uk

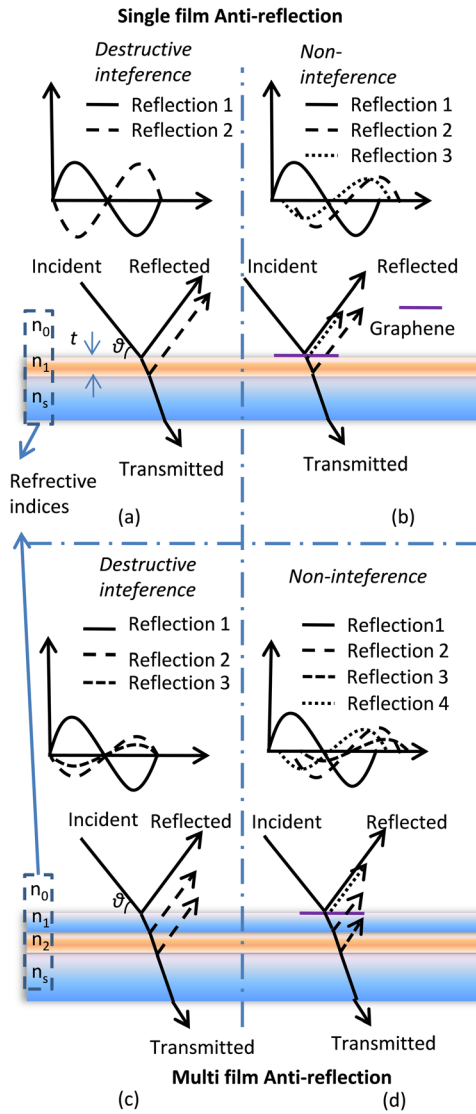


FIG. 1. (Color online) (a) Single layer antireflective film. (b) Graphene which destroys the interference condition of single layer antireflective film. (c) Multilayer antireflective film. (d) Graphene which destroys the interference condition of multilayer antireflective film.

top [Fig. 1(d)], the light cancellation effect will be influenced greatly.

B. Reflectivity of multilayer system

For multilayer optical system, it is much more convenient to use the transfer matrix formulas to calculate the reflectivity.¹² Assuming a m -layer system such as the one shown in Fig. 1(c), the electric field and magnetic field magnitude in the j th layer can be expressed as

$$\begin{bmatrix} E_j \\ H_j \end{bmatrix} = M_1 \cdots M_{j+1} \cdots M_m \begin{bmatrix} E_m \\ H_m \end{bmatrix} = \begin{bmatrix} B \\ C \end{bmatrix}, \quad (1)$$

where E_j and H_j are the electric and magnetic field, respectively, of the j th layer. 0th layer denotes the air, and the m th layer is the substrate. B and C are just the two entries of the result matrix. The product of the M matrices is

$$M = \prod_{j=1}^m M_j = \prod_{j=1}^m \begin{bmatrix} \cos \delta_j & \frac{i}{\eta_j} \sin \delta_j \\ i\eta_j \sin \delta_j & \cos \delta_j \end{bmatrix}, \quad (2)$$

$$\delta_j = \frac{2\pi}{\lambda} N_j d_j \cos \theta_j, \quad (3)$$

where δ_j is the phase shift or optical path induced by the j th layer. N_j is the refractive index of the j th layer, while d_j is the thickness. The equivalent impedance Y of the 0th layer is then

$$Y = \frac{E_0}{H_0} = \frac{B}{C}. \quad (4)$$

And the reflective coefficient τ is

$$\tau = \frac{Y_0 - Y}{Y_0 + Y}. \quad (5)$$

The reflective rate R is then

$$R = \left| \frac{N_0 - Y}{N_0 + Y} \right|^2. \quad (6)$$

There are different ways of defining contrast. We follow Blake *et al.*¹⁰ to define the contrast as

$$c = \left| \frac{R_2 - R_1}{R_1} \right|, \quad (7)$$

where c is the contrast, R_0 is the reflection of substrate, and R is the reflection of the area with graphene.

III. RESULTS AND DISCUSSION

A. Simulation

Reflectivity as well as the contrast has been calculated using the method elaborated above. Since the refractive indices involved are all dispersive over the optical range, the refractive index at an arbitrary point is interpolated from discrete tables.¹³ Graphene has a similar refractive index of bulk graphite 2.6-1.3i, and the thickness of SLG is estimated to be 0.34 nm. Previous reports have verified that these parameters fit the experimental results very well.¹⁰

To achieve the highest visibility of graphene on poly-Si substrate, the thicknesses of both poly-Si and SiO₂ should be optimized. Since the contrast is wavelength dependent, the integral contrast over 400–740 nm has been set as the objective function, with the two thicknesses being parameters. Figure 2 is contour plot of the integral contrast against the thicknesses of both poly-Si and SiO₂. The thicknesses of poly-Si and SiO₂ increase from 20 to 150 nm and from 20 to 350 nm, respectively, in 2 nm a step. When the thickness of the poly-Si is fixed at 75 nm, the integral contrast is increasing and decreasing alternatively with increasing SiO₂ thickness; however, the intensity of the peaks with thicker SiO₂ are weakened due to the dispersion of the reflection with wavelength. A thicker film thickness will make reflective

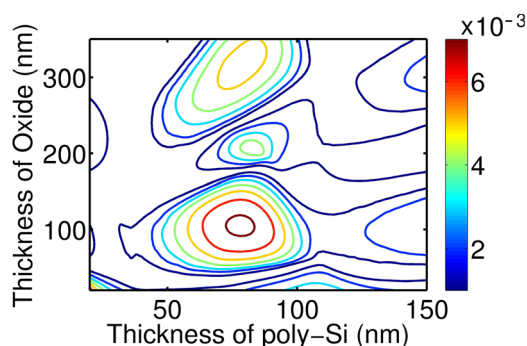


FIG. 2. (Color online) Contour plot over integral contrast in optical range against thicknesses of both poly-Si and SiO₂.

curve more dispersive, therefore, the integral contrast will decrease. Similarly, when the thickness of SiO₂ is fixed, the contrast also falls with thicker poly-Si even more rapidly. Besides the dispersion of reflectivity, the absorption of poly-Si also contributes to the decrease of peak intensities. The thicker the poly-Si film is, the more the light will be attenuated.

It has been found in Fig. 2 that the combination of 75 nm thick poly-Si and 100 nm SiO₂ layer will give a maximum integral contrast. The reflectivity [Fig. 3(a)] and contrast [Fig. 3(b)] as a function of wavelength have been calculated at this point. The maximum contrast is found to be near the wavelength of 600 nm. There is a relatively large range spanning from 580–620 nm where contrast larger than 10% is observed. The inset of Fig. 3(a) shows the detail of the reflection curve around 600 nm. The reflectivity of substrate is smaller than the area covered by SLG, which may be due to the larger refractive index difference at the air/poly-Si

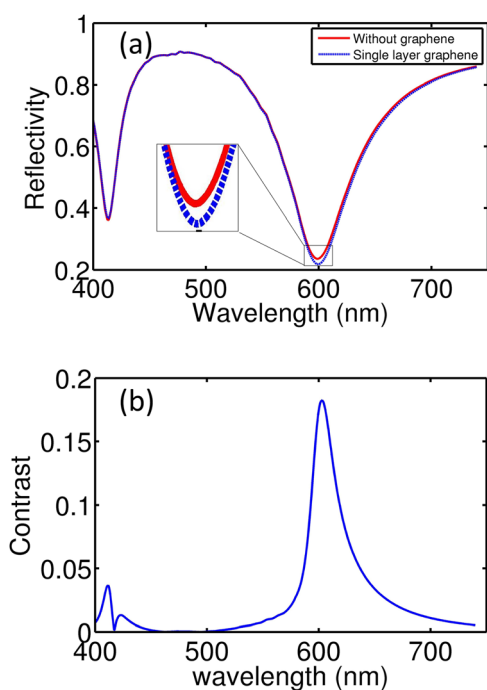


FIG. 3. (Color online) (a) Reflective spectra of 76 nm poly-Si/102 nm SiO₂/Si with (blue dashed) and without (red solid) single layer graphene. (b) Contrast of graphene on the 75 nm poly-Si/102 nm SiO₂/Si substrate.

interface. Since the refractive index difference at the interface of air/poly-Si is bigger than that at the air/graphene interface, the reflectivity of 600 nm light will be higher at the air/poly-Si interface compared to the air/graphene interface, as indicated in the inset of Fig. 3(b). Therefore, the presence of graphene on the poly-Si will cause higher destructive interference, thus decreasing the reflectivity.

It is worth mentioning that it is the integral contrast that has been used as an objective function rather than contrast at one wavelength point. If the single point contrast is used as an objective function, the contrast will be too sensitive to the wavelength as well as the thicknesses of the films. It will not leave enough margins for process errors. Moreover, the possibility of finding an existing narrow band optical at exactly the maximum contrast wavelength will be very low.

B. Experiment

In order to compare the contrast of graphene on widely used 285 nm SiO₂ substrate and the optimized 75 nm poly-Si/100 nm SiO₂/Si multilayer substrate, both of these two types of substrates have been fabricated. First, 100 nm SiO₂ is grown on top of a 4 in. silicon wafer by wet oxidation. Then 75 nm poly-Si layer has been deposited on top of SiO₂ by low pressure chemical vapor deposition (LPCVD). The 285 nm SiO₂ is grown on Si wafer with the same method as for the 100 nm SiO₂.

Graphene grown on Ni catalyst has been transferred to the substrates by the process shown in Fig. 4. First, a piece of thermal release tape (TRT) has been stuck on the graphene [(a) and (b)]. 1 M aqueous FeCl₃ is then used to etch all the nickel away and the tape and graphene will come off together (c). After being rinsed with deionized water and dried with nitrogen gun, the graphene side of graphene/TRT is placed gently on the substrates using tweezer tip to squeeze out the air gradually between substrate and graphene (d). The whole structure is then placed on a hotplate of 100 °C to release the tape (e). To remove the tape residue, the samples have been rinsed in isopropanol, acetone, and deionized water in sequence.

C. Characterization

Figure 5(a) shows the image of graphene sheet on top of the optimized poly-Si/SiO₂/Si substrate under optical microscope with ordinary halogen lamp light, while Fig. 5(b) is image of the same place as (a) but with illumination filtered by narrow band filter (Band pass Filter, 600 ± 2 nm center, 10 ± 2 nm FWHM, Newport Spectra-physics Ltd.). Similarly, Figs. 5(c) and 5(d) are graphene on 285 nm SiO₂ under ordinary and 600 nm illumination, respectively.

In order to verify that the formulae used in the simulation are valid, the simulated reflection spectrum [Fig. 5(a)] has been converted into color vector expressed in red (R), green (G), and blue (B) components by Commission Internationale de l'Éclairage (CIE) color matching function,¹⁴ then compared to the RGB value extracted from ordinary optical image of fabricated substrate as shown in Fig. 5(a). Ideal white light illumination has been assumed for the color

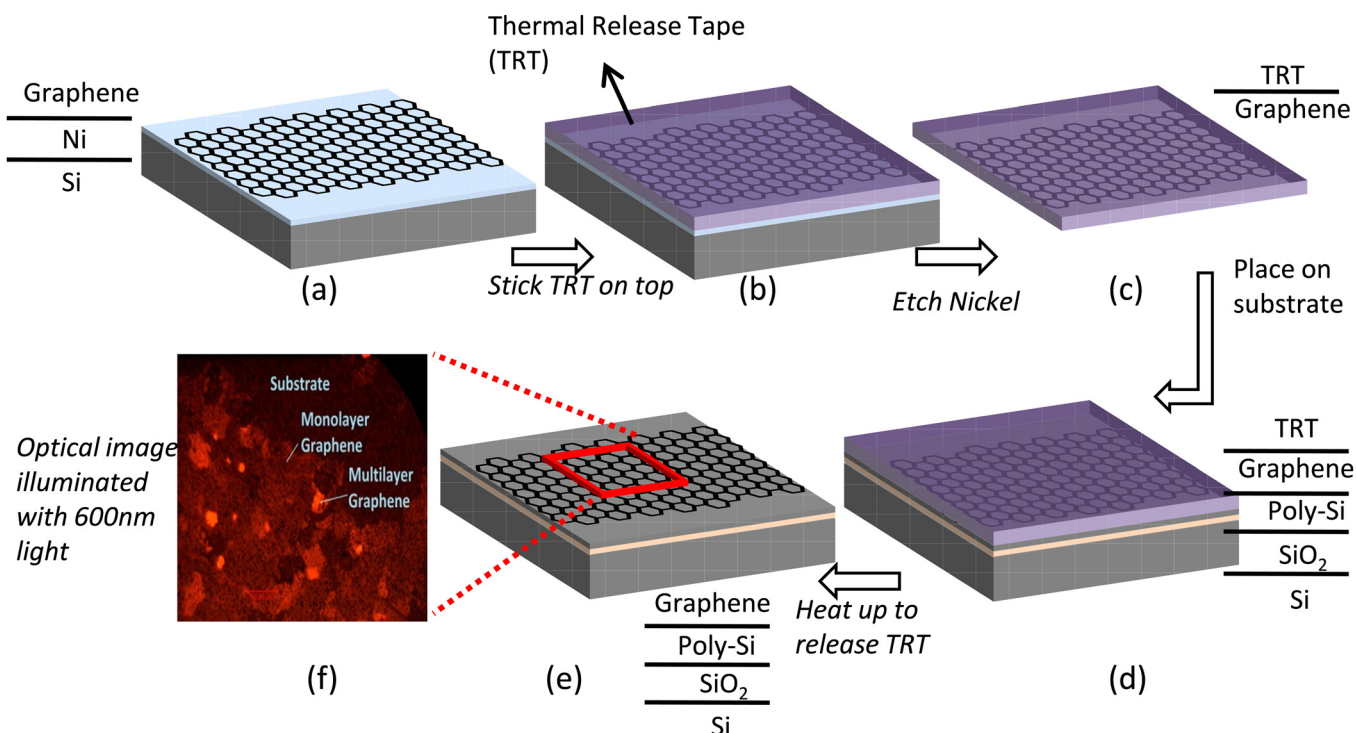


FIG. 4. (Color online) Transferring of graphene onto substrates. (a) CVD grown graphene on Ni catalyst. (b) TRT stuck down to graphene. (c) Etching of Ni in 1 M aqueous FeCl₃ solution. (d) Graphene placed on substrates. (e) Heating up to release TRT. (f) Optical image of CVD grown graphene on poly-Si substrate illuminated with 600 nm wavelength light.

matching. As the illumination intensity affects the absolute RGB values, it is the ratio among the RGB components that is compared. The simulated R : G : B ratio is 0.35 : 0.86 : 1, while the RGB ratio extracted from Fig. 5(a) is

41 : 124 : 154 = 0.27 : 0.81 : 1. The extracted and the simulated R : G : B ratios agree quite well. The small difference between the ratios may come from the difference between spectrum of halogen lamp and the ideal white light spectrum,

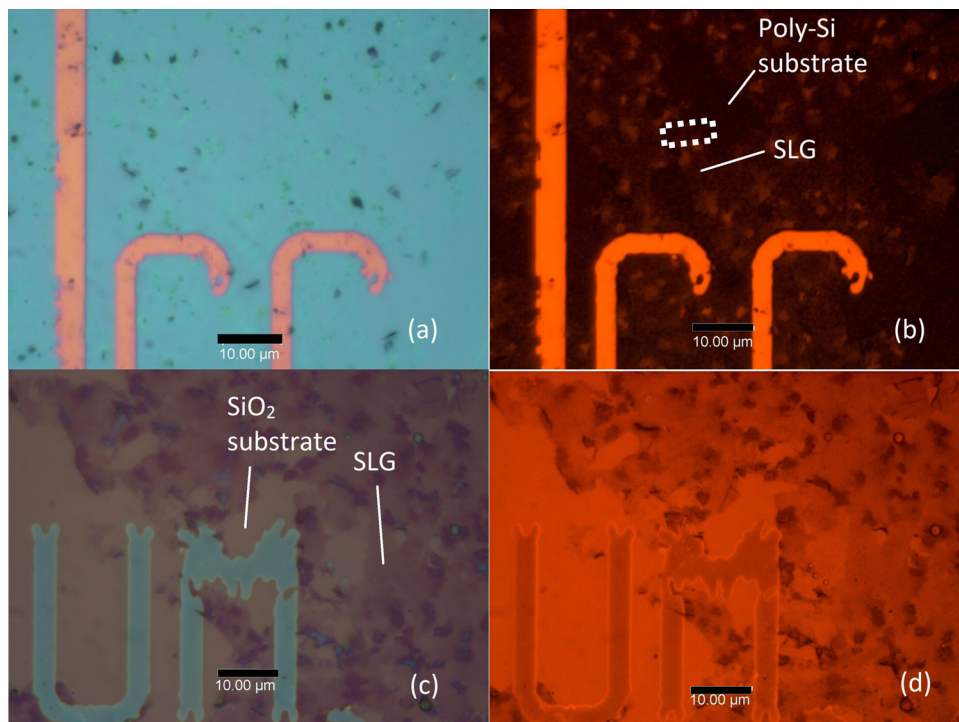


FIG. 5. (Color online) Optical images of graphene on poly-Si substrate (a) and (b) and graphene on SiO₂ substrate (c) and (d). Comparison of (a) and (b) shows that the visibility of graphene has been enhanced at the 600 nm wavelength with the optimized poly-Si/SiO₂/Si substrate. The label SLG in (b) points to a piece of single layer graphene verified by Raman spectroscopy. The poly-Si looks dark as it has been designed to be antireflective. The rectangular area covers both graphene and exposed poly-Si surface to be examined by AFM. The scale is 10 μm.

as well as the diffraction of microscope and light from environment. The comparison of calculated and measured color proves that the simulation has been reliable.

In Fig. 5(a), the graphene is barely seen, but in Fig. 5(b), the SLG (verified by Raman spectroscopy, discussed below), and randomly located multilayer graphene (MLG) are clearly seen. The morphology is consistent with reported graphene grown on nickel.¹⁵ The contrast between the SLG area and the multilayer substrate is 8.7%, large enough to be seen under optical microscope, indicating that the substrate does enhance the visibility of SLG with illumination wavelength of 600 nm. Figure 5(c) is the image of CVD grown graphene on 285 nm SiO₂ illuminated under normal light. The contrast of graphene and the substrate is 6%, slightly increasing to 6.5% when illuminated with filtered light [Fig. 5(d)]. The enhancement of contrast on SiO₂ substrate is very small, complying with the reported contrast against wavelength.¹⁴

It is important to point out that, assuming all surfaces are smooth, the reflection of graphene covered area will be weaker than the substrate according to the simulation, as the refractive index of graphene is closer to air than poly-Si, thus less reflective, while the observed result in Fig. 5(b) is to the contrary. The uncovered poly-Si area is observed to be less reflective. One of the possible causes could be due to the roughness of the surface of CVD grown poly-Si, which scatters away the light; therefore, less light is collected by the objective of the microscope. Figure 6(a) shows atomic force microscope (AFM) image of poly-Si substrate. The root mean-square-average surface roughness R_q of the poly-Si surface is about 2.19 nm, more than double the typical value R_q of crystalline Si wafer, which is less than 1 nm. Figure 6(b) is the AFM image corresponding to the area enclosed in the dotted rectangular in Fig. 5(b), while Fig. 6(c) is the height profile along the line in Fig. 5(b) from right to left, that is to say, from substrate to graphene. Although the height profile is quite rough, a step of about 1.752 nm between graphene and the substrate is clearly identifiable. The roughness of poly-Si surface may also lead to gaps between graphene and poly-Si,

which makes the transfer matrix theory not applicable in this area any more. In summary, although probably the vertical reflection is decreased from the predicted intensity due to surface roughness, and the graphene/poly-Si interface may not fulfill the conditions of transfer matrix theory because of the presumably existing gaps, the requirements of antireflection of the substrate have been fulfilled to allow a significant change of reflection by SLG, hence, the visibility is increased.

A Raman spectrum has been taken at point labeled as SLG in the optical image in Fig. 5(b). To reduce the possible sample heating effect, the laser power has been kept lowest. The wavelength of the laser is 514 nm. Due to the thinness of graphene, the signal to noise ratio (SNR) is very low. Multiple accumulations have been used to increase the SNR. The G band and 2D band are very strong [Fig. 7(a)], which are located at 1580 and 2700 cm⁻¹, respectively. These two bands are the signatures of graphite.¹⁶ The D band, which is attributed to defects, is not obvious in the spectrum. This is consistent with previous reports.^{16,17}

Typically, 2D band originates from double resonance effect,¹⁸ consisting of four peaks for more than two layers graphene, which is due to energy band splitting of both the conduction band and the valence band. The intensity of the four peaks and the shape of 2D band are dependent on the number of layers. In the case of SLG, only one peak in the 2D band can be resolved. Therefore, it is possible to distinguish between SLG and MLG. In our experiment, a closer examination of 2D band [Fig. 7(b)] shows that the band is symmetrical and can be fitted very well with just one Lorentz peak, which confirms that the labeled area is SLG indeed.

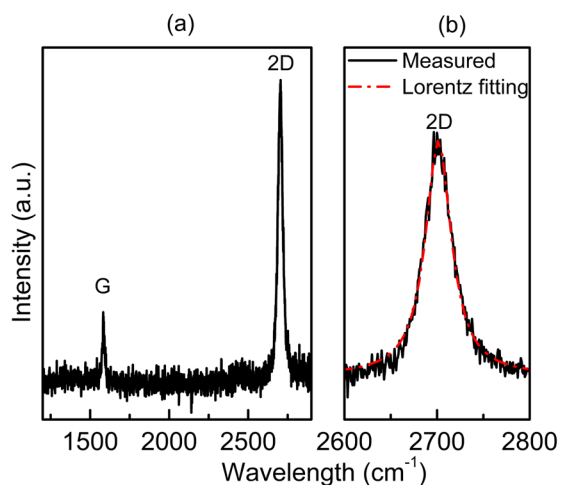


FIG. 6. (Color online) (a) AFM image of poly-Si substrate. The roughness R_q is about 2.19 nm. (b) AFM image of the enclosed rectangular area in Fig. 5(b). (c) Height profile along the line in (b), from right to left.

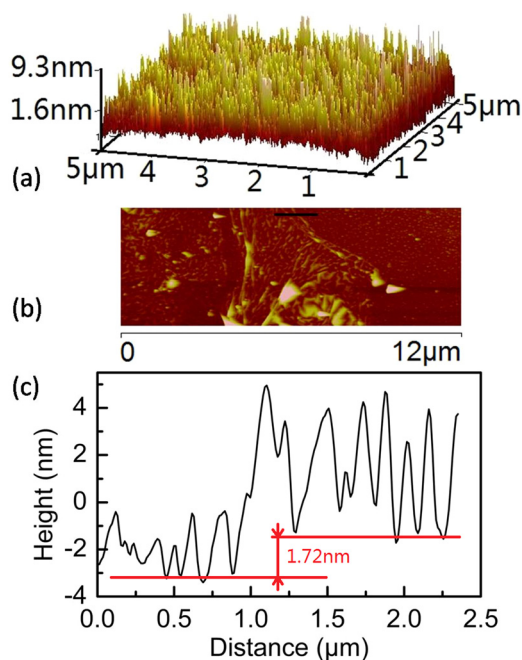


FIG. 7. (Color online) Raman spectrum of the point denoted as SLG in Fig. 5(b). The G peak and 2D peak are located at 1580 and 2700 cm⁻¹, respectively, implying graphene exists at the point, and the symmetrical single peak 2D band proves the graphene is single layer.

IV. CONCLUSIONS

A method of optimizing the visibility of graphene on poly-Si has been developed based on the transfer matrix theory of thin film optics. Contour plot of integral contrast against both thicknesses of poly-Si and SiO₂ has been obtained by parametric study. The optimized thicknesses of both SiO₂ and poly-Si have been found to be 75 and 100 nm, respectively.

The poly-Si/SiO₂/Si structure and ordinary 285 nm SiO₂ substrate have been fabricated. CVD grown graphene has been transferred to the substrates with the aid of thermal release tape. The samples have been examined under illumination of normal halogen lamp and the light filtered by 600 ± 2 nm narrow band optical filter. The contrast of SLG on poly-Si has been enhanced on the 75 nm poly-Si/100 nm SiO₂/Si substrate. Raman spectra have confirmed the number of layers of graphene sheet.

ACKNOWLEDGMENTS

Tao Chen would like to thank the Chinese Scholarship Council for supporting his Ph.D. study, as well as Andrei Gromov and Oleg Nerushev for help with Raman and AFM characterization.

- ¹K. S. Novoselov, A. K. Geim, S. V. Morozov, D. Jiang, Y. Zhang, S. C. Dubonos, I. V. Grigorieva, and A. A. Firsov, *Science* **306**, 666 (2004).
- ²Y. Dan, Y. Lu, N. J. Kybert, Z. Luo, and A. T. C. Johnson, *Nano Lett.* **9**, 1472 (2009).
- ³A. M. van der Zande *et al.*, *Nano Lett.* **10**, 4869 (2010).
- ⁴S. Lee, B. J. Kim, H. Jang, S. C. Yoon, C. Lee, B. H. Hong, J. A. Rogers, J. H. Cho, and J. H. Ahn, *Nano Lett.* **11**, 4642 (2011).
- ⁵V. V. Cheianov and V. I. Fal'ko, *Phys. Rev. B* **74**, 041403(R) (2006).
- ⁶M. Kim, N. S. Safron, C. Huang, M. S. Arnold, and P. Gopalan, *Nano Lett.* **12**, 182 (2012).
- ⁷G. Gu and Z. Xie, *Appl. Phys. Lett.* **98**, 083502 (2011).
- ⁸M. Friedemann, K. Pierz, R. Stosch, and F. J. Ahlers, *Appl. Phys. Lett.* **95**, 102103 (2009).
- ⁹C. Cairaghi, A. Hartschuh, E. Lidorikis, H. Qian, H. Harutyunyan, T. Gokus, K. S. Novoselov, and A. C. Ferrari, *Nano Lett.* **7**, 2011 (2007).
- ¹⁰P. Blake, E. W. Hill, A. H. Castro Neto, K. S. Novoselov, D. Jiang, R. Yang, T. J. Booth, and A. K. Geim, *Appl. Phys. Lett.* **91**, 063124 (2007).
- ¹¹S. Roddaro, P. Pingue, V. Piazza, V. Pellegrini, and F. Beltram, *Nano Lett.* **7**, 2707 (2007).
- ¹²P. J. Leurgans, *J. Opt. Soc. Am.* **41**, 714 (1951).
- ¹³M. J. Weber, *Handbook of Optical Materials* (CRC, Boca Raton, FL, 2003).
- ¹⁴Commission Internationale de l'Éclairage (CIE), Standard on Colorimetric Observers, CIE S002 (1986).
- ¹⁵K. S. Kim *et al.*, *Nature* **457**, 706 (2009).
- ¹⁶A. C. Ferrari, J. C. Meyer, V. Scardaci, C. Casiraghi, M. Lazzeri, F. Mauri, S. Piscanec, and D. Jiang, *Phys. Rev. Lett.* **97**, 187401 (2006).
- ¹⁷L. M. Malard, M. A. Pimenta, G. Dresselhaus, and M. S. Dresselhaus, *Phys. Rep.* **473**, 51 (2009).
- ¹⁸C. Thomsen and S. Reich, *Phys. Rev. Lett.* **85**, 5214 (2000).